Detection and Retrieval of Mineral Dust Aerosol using AERI During the UAE^2 Field Campaign: Application to ARM Measurements

Richard Hansell Jr. (rhansell@atmos.ucla.edu) [1], K.N. Liou [1], S.C. Ou [1], S.C. Tsay [2], J. Ji [2]

[1] Department of Atmospheric and Oceanic Sciences, UCLA

[2] Goddard Space Flight Center, NASA, Greenbelt, Maryland

I Introduction

Quantifying radiative forcing of mineral dust remains a formidable challenge, particularly at long wavelengths due in part to limited IR observational data (Reid et al. 2003)[1] and large uncertainties in modeling dust optical properties (Sokolik et al. 2001)[2]. This study uses data from the GSFC NASA SMART AERI system (Fig.1a-b) to detect and retrieve dust IR optical depths, τ_d (10μm) and effective particle size, R_{eff} during the UAE^2, 2004. Methodology is also applied to AERI data from the ARM Aerosol IOP, 2003. A collocated Raman Lidar and AERONET sun-photometer are used for comparison, however due to the large uncertainties in dust model parameters, further work is required for proper validation efforts.

Fig. 1a. GSFC NASA Surface Measurements Atmospheric Radiative Transfer (SMART) at Al-Ain Airport,UAE, 2004.

Fig. 1b. Atmospheric Emitted Radiation Interferometer (AERI) inside SMART.

II Dust Size,Shape, and Composition (SSC)

This study uses data from the TSI 3321 aerodynamic particle sizer (Fig. 2a) to characterize dust size parameter. Data is re-binned into 6 size distributions N_i according to surface area mean radius given by:

$$\frac{\sum_{i=1}^{50} d_i^2}{n}$$

d_i = central bin radius
n = total particle count
i = APS bins

Effective sizes range from 0.8– 2.0μm. Particle shape distributions (Fig. 2b) are defined to be either idealized spheres (Mie)[3] for comparison, oblate spheroids (T-matrix)[3] with aspect ratio (a/b) = 2, and hexagonal plates (FDTD)[4] with L=a (compact hexagons). Particle composition (Fig. 2c) assumes pure amorphous quartz[5] (SiO_2), montmorillinite[6] ((Na,Ca)(Al,Mg)6(Si4O10)3(OH)6-nH2O),an aggregated mixture of the two minerals using the Bruggeman approximation, and the Volz[7] bulk dust model (mostly illite, kaolinite and quartz traces) from collected dust samples in Barbados.

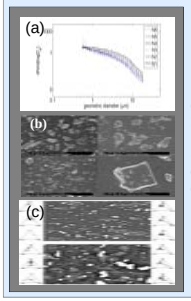

Fig. 2a (6) composite APS size distributions.

Fig. 2b SEM secondary electron image (Reid et al. 2003) showing variable range of particle shapes (PRIDE 2000). Note the dominance of sharp-cornered/angular particles

Fig. 2c SEM backscattered electron image (Reid et al. 2003) depicting heterogeneity of dust mineral composition

III Dust Single Scattering Properties (SSP)

Optical parameters are size integrated using the APS size spectra. A mono-shape distribution is assumed:

$$\beta_{ext} = \int_{a1}^{a2} \sigma_{ext}(a) n(a) da \qquad \omega = \beta_{scat} / \beta_{ext}$$

$$< g >= \frac{\int_{a1}^{a2} g(a) \sigma_{scat}(a) n(a) da}{\int_{a1}^{a2} \sigma_{scat}(a) n(a) da}$$

Plots below show effects of particle shape on retrieved AOT.

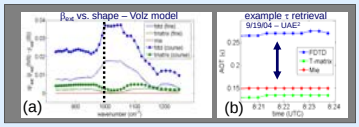

Fig. 3(a) Sensitivity of extinction coefficient (β_{ext}) to particle shape relative to spheres (red line) for fine and coarse mode sizes. Dotted line denotes retrieval (10μm) location.
Fig.3(b) sensitivity of retrieved τ to β_{ext}. Error can be up to 100%

Similarly, sensitivity of composition to dust SSP is large and can effect the retrieved results in excess of 100%. (For example, τ(montmorillinite) > τ(quartz))

IV Detection Methodology

First (17) AERI μ-windows (narrow spectral regions having minimum BT) are selected inside the thermal IR window (800-1200 cm^{-1}).

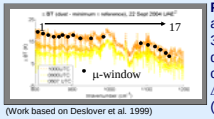

(Work based on Deslover et al. 1999)

Fig. 4a μ-win locations across AERI spectrum. 3 spectra are plotted for different times showing changes in dust loading. ΔBT =AERI (dust) – AERI (clear).

Differences in the IR refractive indices between common earth-based minerals and water/ice are exploited to detect dust from cloud. Silicates display a strong absorption peak (8-10μm). Water/ice, however, are nearly flat in the same spectral range (Fig.4b).

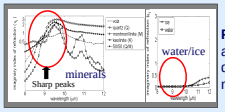

Fig. 4b log plots of absorptive index. Note differences between minerals & water/ice.

Cirrus removed noting BT slope between μ-windows 14 & 15 (Fig. 4c). If BT14 < BT15 → cirrus flag = 1.

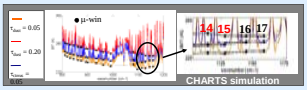

Fig. 4c

Water cloud removed by rejecting spectra when < BT > exceeds 2σ due to large signal of water cloud.

V Retrieval Methodology

CHARTS RTM is used to build LUT of BT's across 17 AERI μ-windows. BT's are computed at AOT (10μm) for τ= 0.05, 0.2, 0.4, 0.6, 0.8 and R_{eff} = 0.8, 1.5 and 2.0μm using a mid-latitude summer atmospheric profile. Points are linearly interpolated to further resolve τ. Temperature corrections are applied to AERI spectra to account for T↑ during the day. Changes in PWV will be addressed in future work. Retrieval employs a statistical optimization approach:

$$\chi^2 = \sum_{i=1}^{17} [\ln(\Delta BT^i_{calc}) - \ln(\Delta BT^i_{aeri})]^2$$

$$\Delta BT = BT_{calc/aeri} - BT_{clear}$$

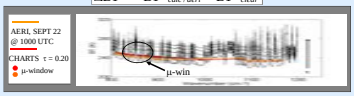

Fig. 5 Calculated AERI BT spectra (black curves) for τ = 0.05, 0.2, 0.4, 0.6, 0.8 (τ ↑ from bottom to top) with R_{eff} = 1.5μm. Dust assumed to be composed of amorphous quartz and spheroidal. Red circles denote calculated μ-win locations. Superimposed for comparison are AERI observed μ-win (orange). Deviations attributed to unknown composition and shape distribution.

VI ARM Results

Dust was observed from 7-9 May, 2003 during the ARM Aerosol IOP. Increased mass measured by a drum impactor (Fig. 6a) suggested soil aerosol. Compositional analysis showed ↑ Ca/Fe ratio common for Saharan dust and back trajectory analysis (Fig. 6b) confirmed Atlantic transport.

Fig. 6a Fig. 6b

Data plots courtesy Thomas A. Cahill and the DELTA Group, University of California, Davis. Made available through ARM data archive

Detection:

May 7/9 are chosen for study. Raman Lidar is used for cloud mask (cm) comparison (Fig. 6c)

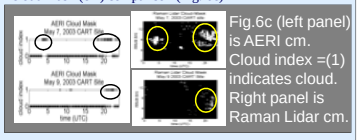

Fig.6c (left panel) is AERI cm. Cloud index =(1) indicates cloud. Right panel is Raman Lidar cm.

Retrieval:

May 9 retrieval (6-hour period) is shown below (Fig.6d left) using a Volz -spheroidal model. Raman lidar β_{ext} (right) at 0.3μm for same time period is shown for comparison. Note larger AERI τ (red circle) compared to elevated β_{ext} (black) for 4-hr period then drops to a minimum. Particle size shows dominant coarse mode. Oscillation of size parameter during first 2-hrs is subject to investigation.

Fig.6d

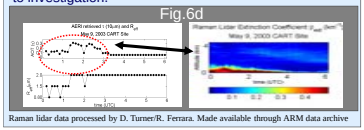

Raman lidar data processed by D. Turner/R. Ferrara. Made available through ARM data archive

VII UAE^2 Results

UAE^2 was conducted from Aug-Oct, 2004 in UAE. The NASA SMART system, located at Al-Ain Airport, housed the AERI instrument. Collocated instruments used for comparison include AERONET and the micro-pulse lidar (MPL). Shown below (Fig. 7a) is an AERI retrieval for 9/19/2004. Fig. 7b compares the AERI τ (10μm) to AERONET τ (0.55μm) after applying the theoretical quartz β_{ext}(0.55 μm)/ β_{ext}(10 μm) correction, which tends to ~ 2 for the size parameters considered. The MPL image (Fig. 7c) depicts elevated dust around 1100-1300(UTC). Increases in retrieved τ (both instruments) occur during this dust transit.

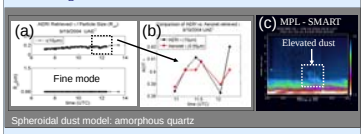

Spheroidal dust model: amorphous quartz

Retrieved particle size shows dominant fine mode. Total (fine + coarse mode) averaged volume effective radius (AERONET spherical almucantar retrieval) for 9/18 ~ 0.621μm (caution warranted in data interpretation due to retrieval differences !)

VIII Summary

- Uncertainties in particle shapes/composition currently limit retrieval accuracy.
- Retrieved τ for the days/times considered appear reasonable compared to collocated instruments. A more resolved particle size look-up will eliminate jumps in R_{eff} solution.
- Future works include:
  - Add PWV corrections to retrieval
  - Increase atmospheric profiles in LUT to account for complete IR sensitivity to all atmospheric variables.
  - Analyze UAE^2 particle in-situ data (IPA) to help improve modeled dust optical properties.

References:

1. Reid, J.S. , JGR, Vol.108,2003
2. Sokolik, I.N.,JGR,Vol.106,18015-18027,2001
3. Mischenko,M.I.,Appl.Opt.33,7206-7225,1994
4. Yang,P.,Liou,K.N.,Appl.Opt.,3727-3737,2000
5. Popova,S.I.,Optika Spektrosc,v.33,801-803,1972
6. Roush, T.,Icarus,94,191-208,1991
7. Volz,F.E.,Appl.Opt.,12,564-568,1973